

Numerical Simulation of Vortex Rope Formation and Pressure Oscillation in Francis Turbine

Chandan Kumar Sah ^a, Bikki Chhantyal ^a, Binod Singh ^a,
Aabhushan Regmi ^a, Rajendra Shrestha ^a

^a Department of Mechanical Engineering, IOE, Pulchowk Campus

Corresponding Email: ^a chhantyalbikki@gmail.com

Abstract

Francis turbines are designed to operate at a particular flow rate called the Best Efficiency point (BEP) and operation of turbine at flow rates away from the BEP not only decreases its efficiency but also shortens the life of turbine due to formation of flow instabilities, pressure oscillations and cavitation bubbles. The purpose of this study is to numerically investigate the behavior of flow through the simplified Francis turbine at 0.5 BEP and 0.85 BEP (50% and 85% of the Best efficiency flow rate respectively). Transient simulation, carried out using DES turbulence model indicated the formation of roughly axi symmetrical precessing vortex rope at 0.85 BEP whereas the formation of double helical precessing vortex rope at 0.5 BEP flow rate indicating more regular flow at flow rates closer to BEP. The velocity profile and streamlines of flow inside the draft tube indicated that the vortex rope is formed due to roll up of shear layer at interface of inner low velocity stagnation region and outer high swirl flow. Further, increase in the ratio of azimuthal to axial velocity at 0.5 BEP compared to 0.85 BEP due to increased residual swirl causes vortex breakdown, which is more prominent at 0.5 BEP flow rate. The comparison of pressure amplitude at observation points showed that the amplitude of pressure oscillation increased along radial direction, while it decreased along the axial direction (along the flow). Also, the maximum amplitude of pressure oscillation is found at runner outlet near the draft tube wall. The comparative study of two flow rates indicated more severe pressure oscillations at 0.5 BEP than 0.85 BEP.

Keywords

best efficiency point, flow instabilities, Pressure oscillations, Vortex Breakdown, vortex rope, DES turbulence model, double helical, streamlines, draft tube

1. Introduction

Francis turbine, a mixed type, is one of the most used turbines in hydro power generation. The torque in the runner is imparted due to impact from the water and lift due to pressure difference between top and bottom side of the runner. The torque results in the motion of runner. Usually, the turbine is designed to operate at a given flow rate, but, since the operating flow rate of the turbine varies according to the season, it has to operate far from design flow condition. This in turn subjects the turbine to flow instabilities and swirling flow in draft tube called vortex rope [1], whose instability along the draft tube leads to vortex breakdown [2].

The vortex rope problem is well known phenomenon and can be mitigated in different ways. Active method where additional energy is used and the other, passive

method, where additional energy is not used. The passive methods includes fins mounted in the cone [3], extending cones mounted in runner's crown [4] or using J-grooves [5]. The active method includes water injection [6] and air injection [7]. The air admission is used when the pressure level in the turbine is lower than atmospheric pressure. In this case, the air is sucked without any additional energy. Contrary, an external energy source is required in order to inject air when the pressure level in the turbine is higher than atmospheric one. Therefore, it is required to be known the pressure distribution in the draft tube.

The pressure oscillation results in the mechanical vibration. If the frequency of oscillation matches the natural frequency of the structures, resonance occurs, at which, whole system vibrates with high amplitude, which has got detrimental effects, so this need to be

avoided. The pressure distribution is necessary to get an idea about location and quantity of dampening.

Due to rapid fluctuation of pressure at part load condition, the small vapor filled bubbles are formed. These bubbles collapse in interaction with structure and create intense shock wave which leads to structural damage. It is called cavitation. The high pressurized air is injected to reduce this phenomenon. The pressure distribution is necessary to locate the cavitation prone areas and hence injection method and angle.

This paper presents numerical simulation of the flow through the draft tube at different part load conditions, 0.5 BEP and 0.85 BEP to find the corresponding nature of vortex rope and pressure distribution at different investigation points. For the transient simulation, DES turbulence model is used whose result better aligns with the experimental results.

2. Methodology

The objective of this study is to numerically investigate the flow through a Francis turbine, and numerical simulation requires appropriate modeling of the turbine fluid domain, which was attained using SolidWorks software. The required engineering drawings for modeling of the turbine were obtained from Middle Marsyangdi Hydropower Station and in order to extrapolate the angle of gate opening of wicket gates at 0.5 BEP and 0.85 BEP, data of percentage gate opening with flow rate was also obtained from the control room of the Station. Figure 1 is the regression plot of angle of wicket gate versus flow rate, which is plotted from data obtained from the station. From the plot, the angle of guide vanes at 0.5 BEP and 0.85 BEP flow rates can be interpolated which is used for modeling the Francis turbine at required guide vanes angle for respective flow rates.

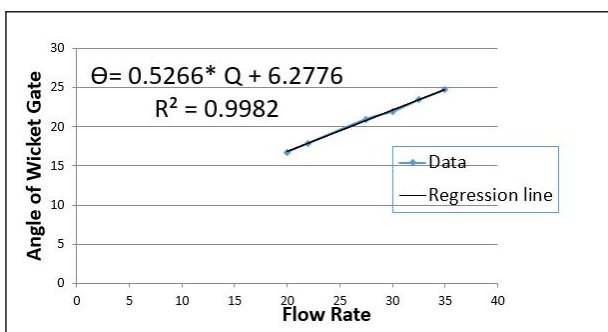


Figure 1: Angle of wicket gate vs flow rate

For literature review available course books, websites, thesis reports, journals and research papers were referred. The validation of different turbulence models with experimental results doesn't lie within the scope of this research so valid turbulence models were chosen from literature. After the appropriately simplified fluid domains were created, the model was imported to Pointwise software for meshing and then simulations were carried out using ANSYS fluent.

3. Numerical Simulation

3.1 Turbulence Model and Governing Equation

Shear Stress Transport (SST) k - ω based Detached Eddy Simulation (DES) turbulence model is used in the simulation. DES turbulence model is used mostly for separated flow with high Reynolds number. It is hybrid turbulence model which models fluid flow with Unsteady Reynolds Averaged Navier Stokes (URANS) in boundary layer and free shear layer with Large Eddy Simulation (LES).

In the flow along the draft tube, the phenomena like vortex breakdown and formation of special pressure pulsation zones (SPPZ) forms at part load condition which is better modeled by DES model. The result by this model is closer to experimental results than URANS [8]. Also, its computational cost is lesser than that of LES which is important criteria for us. Transport Equation for SST $k - \omega$ model [9].

Turbulence kinetic energy:

$$\frac{\partial}{\partial t}(\rho k) + \frac{\partial}{\partial x_i}(\rho k u_i) = \frac{\partial}{\partial x_j}(\Gamma_k \frac{\partial k}{\partial x_j}) + G_k - Y_k + S_k$$

Specific dissipation rate:

$$\frac{\partial}{\partial t}(\rho \omega) + \frac{\partial}{\partial x_i}(\rho \omega u_i) = \frac{\partial}{\partial x_j}(\Gamma_\omega \frac{\partial \omega}{\partial x_j}) + G_\omega - Y_\omega + D_\omega + S_\omega$$

In DES;

$$Y_k = \rho \beta^* k \omega F_{DES}$$

$$F_{DES} = \max(\frac{L_t}{\Delta C_{DES}}, 1)$$

$$L_t = \frac{\sqrt{k}}{\beta \omega}$$

L_t is the turbulence length.

Δ is maximum local grid spacing.

3.2 Geometry and Computational Grids

3.2.1 Modeling

With the help of engineering drawing obtained from the hydropower station, the model was developed in SolidWorks as accurately as possible. The structure comprised of Spiral Casing, Stay rings, wicket gates, runner and the draft tube. And in CFD analysis the only region of concern is the void region: interior part of turbine where the fluid actually flows, so, the void region minus the structural component, which forms the interior is the domain used in the analysis. Spiral casing was not included in the fluid domain to lower the total element count which in turn lowered down the computational power required.

The parameters of the Turbine are listed in table.

Table 1: Parameters of the turbine

SN	Parameters	Value
1	Rated Output Power (MW)	35.9
2	Rated Head (m)	98
3	Rated Speed (rpm)	333.33
4	Rated Discharge (m ³ /s)	40
5	Number of Runner Blades	13
6	Number of Wicket Gates	24
7	Number of Stay Rings	24
8	Inlet Area of Draft Tube (m ²)	4
9	Outlet Area of Draft Tube (m ²)	11.79

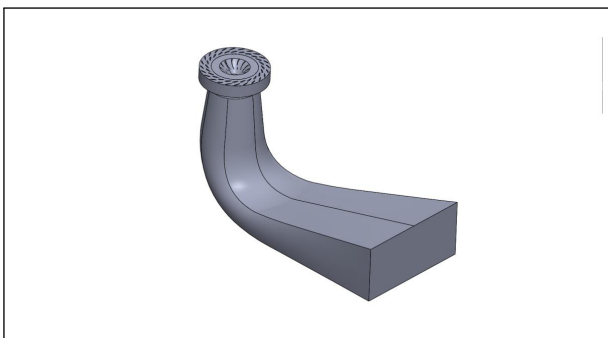


Figure 2: Fluid Domain

3.2.2 Computational Grid

The whole fluid domain was then decomposed into smaller finite control volumes in Pointwise meshing software. Except for runner domain, for which high quality unstructured hybrid mesh with T-Rex feature to grow high quality anisotropic layer from the walls of unstructured domain, structured hexahedral mesh was generated. The Hexahedral Element count was 6,300,084, and the unstructured section of runner

comprised of 1,24,261 tetrahedrons, 111,002 pyramids and 1,889,580 prims, totaling the element count to 9,720,927. For all the generated mesh, the thickness of the first cell from wall is maintained at 1mm, keeping the y+ value in check at around 0.63. Normally, it is advised to have this number down for the accuracy of the turbulence models used, but in doing so would increase the element count hence, increasing the already limited computational power.

The maximum equiangle skewness of the mesh was found to be 0.979, which is lower than the limit imposed by fluent solver. The overall quality of mesh was good for structured mesh, and for unstructured mesh, a few of the elements' skewness exceed 0.8.

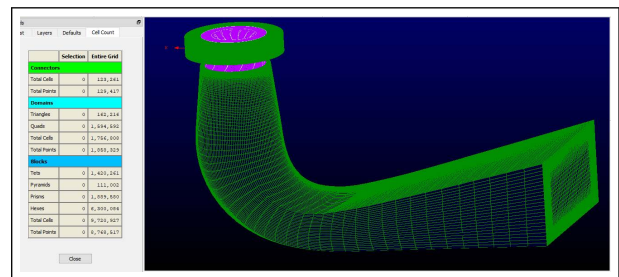


Figure 3: Fluid Domain Mesh

The mesh independent test was performed next. To check whether the result depended on total number of element count, a steady state analysis was performed. For simplicity, the torque of the runner was used as a parameter of interest to carry out mesh independent test. As shown in the chart below the values of torque starts to stabilize when the element count is around 8.7 million, showing the result obtained from our used element count of 9,720,927 is independent to it, hence showing mesh independence. Due to lack of computational power and ensuring mesh independence, the element count of 9,720,927 is taken as final number of element for the further computational simulation.

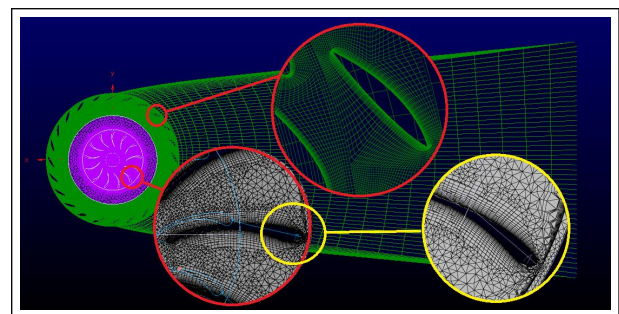


Figure 4: Fine mesh around walls

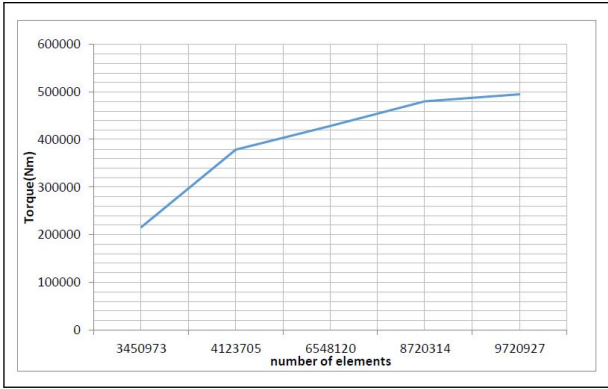


Figure 5: Mesh Independence

3.3 Boundary Condition and Set Up

For the simplicity of computation and reduce the number of cell counts which reduces the computational power required, the spiral casing wasn't part of the fluid domain, instead, the outer cylindrical surface of the stay rings was the velocity inlet surface for both simulations at 0.5 BEP and 0.85 BEP and the inlet velocity was calculated from the data of flow rate at each discharge assuming constant flow through the cylindrical surface. As the inlet angle to the stay rings need to be along the direction of the stay rings blades, cylindrical velocity components were used to define required velocity with runner center being the origin of coordinate system so as to define the constant radial and azimuthal velocity components at inlet as shown in the figure 6.

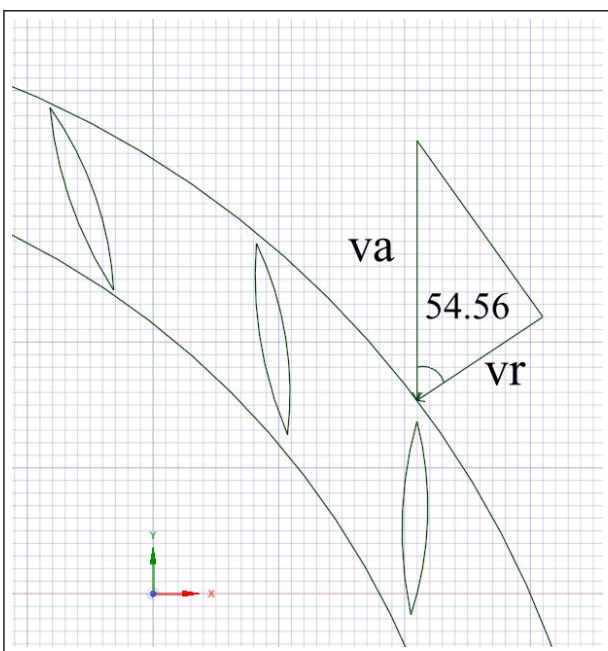


Figure 6: Inlet conditions of velocity

Table below shows the radial and azimuthal components of velocity for 0.5 and 0.85 BEP discharge.

Table 2: Parameters of the turbine

Parameters	0.85 BEP	0.5 BEP
Flow rate(m ³ /s)	34	20
Guide vane velocity(m/s)	6.44	5.007
Guide vane angle(°)	54.56	54.56
Radial velocity(m/s)	3.734	2.903
Azimuthal velocity(m/s)	5.246	4.08
Axial velocity(m/s)	0	0

The outlet of the draft tube was designated pressure outlet defined at 0 atm gauge pressure.

The runner domain forms a fluid domain rotating at 333.33 rpm, hence this behavior was simulated using frame motion for steady state simulation and mesh motion for transient case. The transient simulation was simulated using the DES turbulence model with time step equal to the rotation of runner blade by 1 degree equaling to 5×10^{-4} seconds. Initially, default settings were implemented for simulations as they are robust and unlikely to diverge, later on higher order discretization schemes were used for better results.

4. Results

4.1 Nature of Draft Tube Flow

Figure 7 and 8 show the streamlines pattern of flow inside the Francis turbine at 0.5 and 0.85 BEP. In general, the flow exiting the runner has high circumferential velocity compared to axial velocity as can be evident from the spiraling shape of streamlines in cone of draft tube. As can be seen from the figures 7 and 8, the swirling is higher for flow at 0.5 BEP than that compared to 0.85 BEP and also the former has more irregularities in flow signifying instability around the elbow of the draft tube. In general, at part load condition, the guide vanes angle increases (with respect to radial direction) so as to keep rpm constant, this increase in angle imparts more circulation to the fluid. This mismatch in swirl generated by the guide vanes and angular momentum extracted by the runner of the turbine leads to swirling flow in the draft tube. The main function of the draft tube is to convert the kinetic energy of the flow exiting the runner to static pressure energy hence its the diverging shape. In order for the turbine to extract pressure energy from

kinetic energy of fluid with minimum hydraulic losses, a small amount of swirl is necessary at cone inlet which aids in delaying flow separation in the draft tube assisting pressure recovery. This amount of swirl is tuned for optimal performance at certain flow rate called best efficiency flow rate at which the efficiency is the highest. At other discharge, the value of swirl departs significantly from that at optimal performance point hence efficiency is lower. High swirl intensities evident at lower discharge degraded the performance of the turbine by forming recirculation regions characterized by flow reversal.

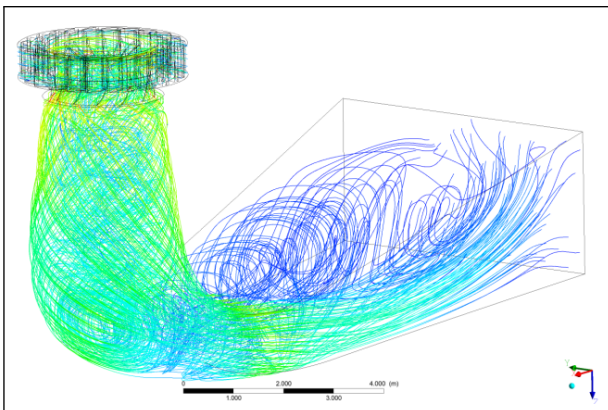


Figure 7: Streamlines at 0.5 BEP

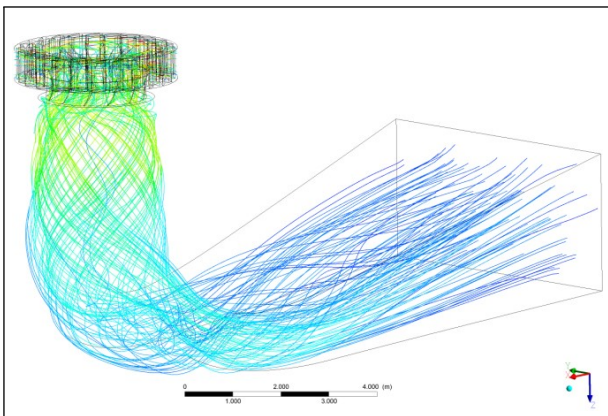


Figure 8: Streamlines at 0.85 BEP

Figures 9 and 10 show the velocity contours of flow in meridian half plane of the turbine for 0.85 BEP and 0.5 BEP obtained from the steady state simulation. The velocity plots show a region of very low velocity in the elbow section of the draft tube just exiting the runner whereas the flow surrounding it has high velocity. The region of low velocity is called stagnation region which is characterized by recirculation regions within the core flow. The stagnation region in the cone of draft tube for 0.85 BEP, though being a 3D region, can

be quantized to extend from runner outlet to elbow section of draft tube whereas that at 0.5 BEP case is more complex in shape so its whole structure cannot be observed by velocity plot in a plane. The shape of the vortex rope formed at respective discharge can provide some insight into the actual 3D shape of stagnation region. As can be seen from the streamlines at the cone of the draft tube, flow reversal and recirculation region within core flow is more prominent at 0.5 BEP compared to 0.85 BEP flow.

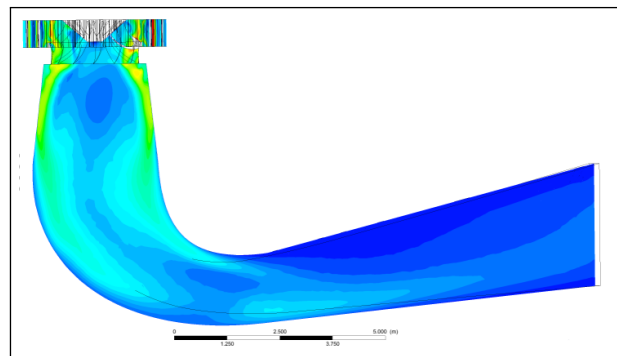


Figure 9: velocity contour in meridional plane for 0.5 BEP flow rate

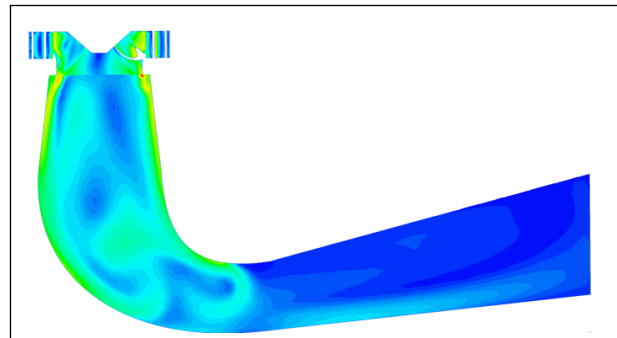


Figure 10: velocity contour in meridional plane for 0.85 BEP flow rate

Figures 11 and 12 are also velocity contours of flow exiting the turbine on a plane. The location of plane is offset at a distance of 2.53 m from the inlet of the draft tube. The stagnation center is exactly at the middle in case of 0.5 resulting in circular void region in the middle. The distribution of velocity is almost axisymmetric in this case. Unlike in 0.5 BEP case, in 0.85 case the stagnation region is displaced to side forming non circular and small stagnation region at the middle. And there is strip of stagnation region formed near wall of draft tube.

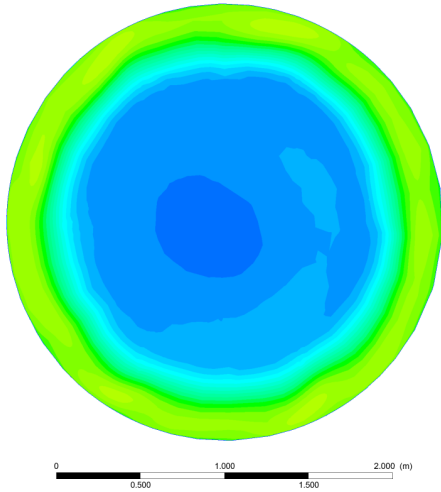


Figure 11: velocity contour on plane $z=2.53\text{m}$ at 0.5 BEP

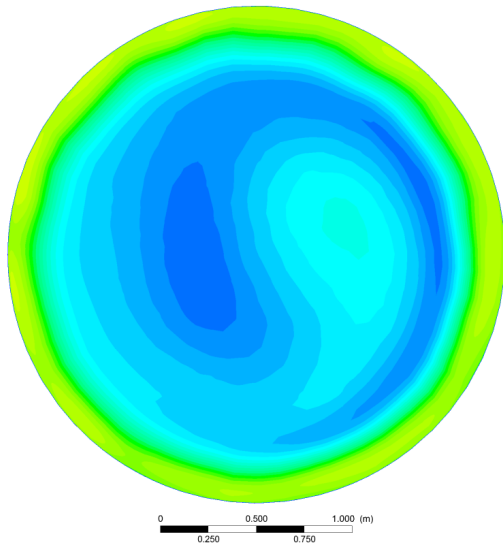


Figure 12: velocity contour on plane $z=2.53\text{m}$ at 0.85 BEP

Figures 13 and 14 show the nature of vortex rope for 0.85 BEP and 0.5 BEP which is plot of iso-pressure surface which is obtained from transient simulation using DES turbulence model. The precessing vortex rope is more prominent at partial flow rate (0.5BEP) forming a near double helical shape whereas at 0.85 BEP, it is roughly axisymmetric. The formation of the vortex rope can be accounted to the roll up of the shear layer at the interface of low velocity inner stagnation region and the outer high velocity swirling flow. This roll up region is quite stable and roughly axisymmetric at flow conditions near BEP and tends to become more unstable as the flow rate decreases from BEP causing vortex breakdown.

For this axisymmetric vortex, a core of high vorticity and appreciable axial velocity is surrounded by high axial velocity fluid. As the spiraling fluid is followed along the axial direction, the structure of vortex rope, indicated by the velocity distribution changes only a slowly at first, and then abruptly, characterized by sudden retardation and recirculation of fluid along the axis. This effect of abrupt change in structure of vortex rope is more pronounced at low discharge. The property of vortex rope formed depends upon a number of factors, mainly depending upon the ratio of azimuthal to axial velocity components at the draft tube cone. The tendency of vortex breakdown is more pronounced for higher value of ratio of azimuthal to axial velocity. Due to the diverging shape of draft tube, the flow along it is retarding, increasing the ratio along the flow. This explains the abrupt change in the velocity and structure of vortex following slow change. Vortex breakdown can be evident in figures 13 and 14, the abrupt breakdown in the structure of vortex rope around the exit to the cone of the draft tube.

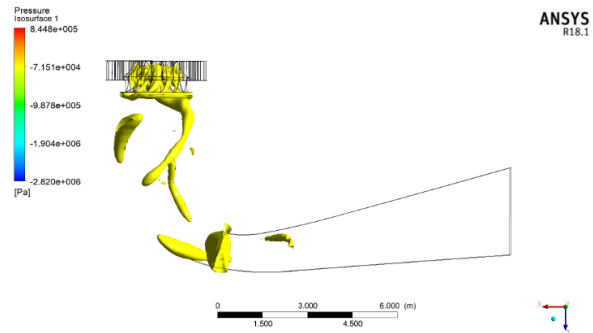


Figure 13: iso-pressure surface of vortex rope at 0.5 BEP

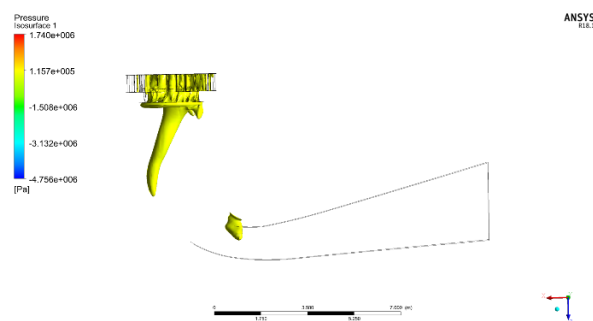


Figure 14: iso-pressure surface of vortex rope at 0.85 BEP

4.2 Pressure Oscillation

The swirl imparted by the runner to the fluid entering the draft tube is necessary for efficient pressure recovery and the amount of swirl imparted is tuned so that efficiency is maximum at BEP. When operated at part load condition, the swirl imparted by the runner exceeds that of BEP. As mentioned earlier, the vortex rope is formed due to roll up of shear layer at the interface of stagnation region and high swirl flow enclosing it. This precessing nature of the double helical vortex rope induces pressure fluctuations within the draft tube. Moreover, severe pressure oscillations cause problem in stable operation of turbine and also power swing in the turbine output.

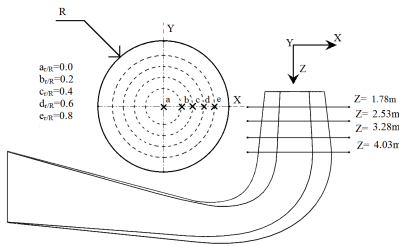


Figure 15: observation points

The pressure oscillations data was taken at twenty points as shown in figure 15. The four non-dimensionalized points along the axis of the draft tube and five non dimensionalized points along the radius. For the first axial location, the pressure oscillation in both amplitude and frequency increased along the radius as can be seen in the figure 16, similar was the case for other axial points. From this observation, it can be inferred that pressure oscillations increase along the radial direction and is maximum at draft tube wall. The dynamic response of pressure for different radial points for first axial location are below:

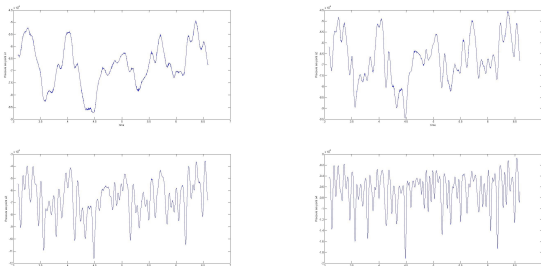


Figure 16: Pressure oscillation along radial direction at points a1, a2, a3 and a4 respectively

The dynamic pressure response along the radial direction is observable because of distinct frequency and amplitude. Whereas, to elucidate comparison between pressure oscillation at draft tube wall along the axial locations, the dynamic response is transformed to frequency response using Fourier transformation.

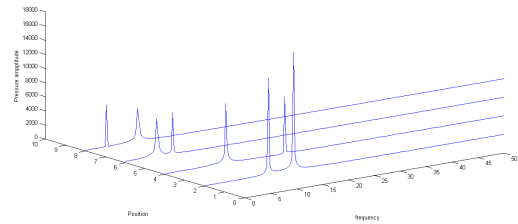


Figure 17: pressure oscillation along axial position from draft tube wall

The above plot shows the frequency and amplitude of pressure oscillation at different axial location. At the axial location closest to the runner, both the amplitude and frequency are greater, so the draft tube vibration will be maximum at this point which may also induce vibrations to the runner. Along the axial locations below it, the amplitude and frequency are decreasing as can be observed in the figure 18.

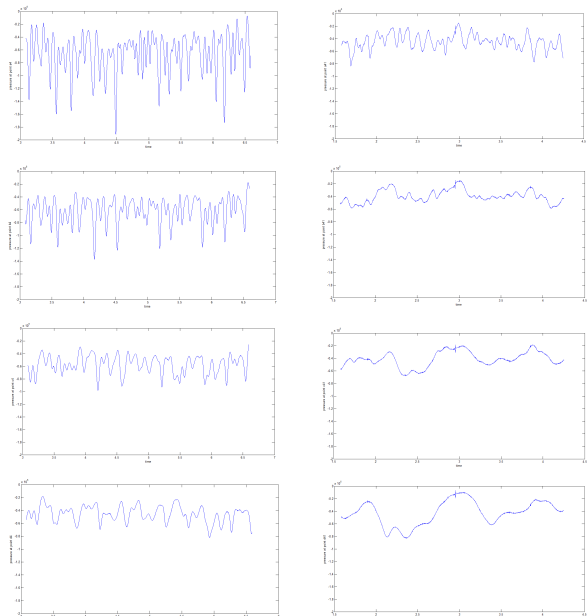


Figure 18: Pressure oscillation comparison for 0.5(left) and 0.85(right) BEP at points a4, b4, c4 and d4 respectively from top to bottom

The pressure oscillations decrease significantly at 0.85 BEP compared to 0.5 BEP. To make comparison, one

wall draft tube pressure is observed for 50% BEP and 85% BEP flow rates. The comparison shows that the amplitude and frequency of oscillation decreased downstream along axial direction from runner outlet.

5. Conclusion

It is found that the formation of double helical precessing vortex rope at 0.85 BEP whereas roughly axi-symmetrical precessing vortex rope indicates that a vortex rope is more prominent at lower flow rates. In addition, it can be inferred from the abrupt breakdown of vortex rope at 0.5 BEP compared to 0.85 BEP that the flow is more unstable and irregular at lower flow rates.

The amplitude as well as frequency of Pressure oscillation is maximum near cone wall for same axial distance from the runner. The oscillation decreases along the axial direction hence, is maximum at the outlet of the runner which implies that the structural vibration will be maximum at this region and requires damping. The pressure fluctuation is low at 0.85 BEP compared to 0.5 BEP. Hence, the pressure oscillation reduces while operating near BEP. So, the turbine is more susceptible to pressure induced vibrations while operating at lower flow rates compared to operations near BEP.

Acknowledgement

The authors express their deepest gratitude towards Middle Marsyangdi Hydropower Plant (MMHP), Station Chief Er. Pasupati Gautam, Senior Er. Atmesh Poudyal for granting the permission to study the Installed Turbine system, their continual support in terms of providing engineering drawings of the system installed, and for the guidance received during stay at the plant. The authors are highly indebted to Asst. Prof. Hari Bahadur Dura, Asst. Prof. Kamal Darlami, Department of Mechanical Engineering, Pulchowk Campus who provided necessary support and guidance and also encouraged and motivated through every step of the research.

References

- [1] Albert Ruprecht, Thomas Helmrich, Thomas Aschenbrenner, and Thomas Scherer. Simulation of vortex rope in a turbine draft tube. In *Proceedings of 22nd IAHR Symposium on Hydraulic Machinery and Systems*, pages 9–12, 2002.
- [2] MG Hall. Vortex breakdown. *Annual review of fluid mechanics*, 4(1):195–218, 1972.
- [3] Michihiro Nishi, XM Wang, K Yoshida, T Takahashi, and T Tsukamoto. An experimental study on fins, their role in control of the draft tube surging. In *Hydraulic Machinery and Cavitation*, pages 905–914. Springer, 1996.
- [4] Thomas Vekve. An experimental investigation of draft tube flow. 2004.
- [5] J KUROKWA. Suppression of swirl in a conical diffuser by use of j-groove. In *Proc. 20th IAHR Symp. CD-ROM*, pages 1–10, 2000.
- [6] Alin Ilie Bosioc, Romeo Susan-Resiga, Sebastian Muntean, and Constantin Tanasa. Unsteady pressure analysis of a swirling flow with vortex rope and axial water injection in a discharge cone. *Journal of Fluids Engineering*, 134(8):081104, 2012.
- [7] Zhong-dong Qian, Jian-dong Yang, and Wen-xin Huai. Numerical simulation and analysis of pressure pulsation in francis hydraulic turbine with air admission. *Journal of Hydrodynamics, Ser. B*, 19(4):467–472, 2007.
- [8] Hosein Foroutan and Savas Yavuzkurt. Flow in the simplified draft tube of a francis turbine operating at partial load—part i: Simulation of the vortex rope. *Journal of Applied Mechanics*, 81(6):061010, 2014.
- [9] Florian R Menter. Two-equation eddy-viscosity turbulence models for engineering applications. *AIAA journal*, 32(8):1598–1605, 1994.